IDMA for Low-Latency and Massive Connectivity over 6G Non-Terrestrial Networks

Yong-Jin Song, Young-Seok Lee, and Bang Chul Jung†
Department of Artificial Intelligence Convergence Network, Ajou University, Suwon, 16499, South Korea
†Department of Electrical and Computer Engineering, Ajou University, Suwon, 16499, South Korea
Email: wiclyjsong@ajou.ac.kr, youngseoklee@ajou.ac.kr, bcjung@ajou.ac.kr

***Abstract*—In this paper, we propose a novel orthogonal frequency-division multiplexing (OFDM)-based interleave-division multiple access (IDMA) technique for non-terrestrial Internet-of-Things (IoT) networks utilizing low Earth orbit (LEO) satellites. Specifically, considering the direct links between LEO satellites and IoT devices, we tailor the IDMA framework by incorporating repetition to ensure stable performance even under severe path loss conditions. Furthermore, in accordance with the adoption of OFDM, which is expected to play a key role in sixth-generation (6G) mobile communications, we conducted practical simulations incorporating channel coding to verify the applicability of IDMA to non-terrestrial networks (NTNs). To enhance the reliability of performance evaluation, channel modeling was established based on standard-compliant NTN specifications. The comprehensive performance analysis confirms that IDMA provides stable and reliable multiple access, indicating its potential as a promising solution for future 6G non-terrestrial IoT networks.**

***Index Terms*—6G, non-terrestrial network (NTN) low Earth orbit (LEO) satellite, Internet-of-Things (IoT), interleave-division multiple access (IDMA), orthogonal frequency-division multiplexing (OFDM), channel coding.**

I. Introduction

The Internet-of-Things (IoT) has emerged as a key wireless technology to realize innovative services, including smart cities, smart homes, remote healthcare, smart transportation, and smart factories [1]. The number of globally connected IoT devices reached 16.6 billion in 2023, representing a 15% year-over-year increase, and is projected to grow to 40 billion by 2030 [2]. The sixth-generation (6G) mobile communication systems, defined in International Mobile Telecommunications (IMT)-2030, aim to achieve a connection density of 10^7 to 10^8 devices per square kilometer. In addition, they introduce global coverage as a new key performance indicator, thereby outlining a direction for service evolution toward large-scale connectivity. To this end, non-terrestrial networks (NTNs) utilizing satellites have recently attracted significant attention as a promising solution not only for providing global coverage but also for extending communication services to maritime, aeronautical, and disaster areas [3]. In other words, the adoption of NTNs complements the limitations of existing terrestrial infrastructures and is emerging as a key technology to enable seamless connectivity anytime and anywhere.

NTNs constitute a global networking architecture that includes geostationary Earth orbit (GEO), medium EO (MEO), and low EO (LEO) satellites, as well as high-altitude platforms (HAPs) and unmanned aerial vehicles (UAVs). Among these platforms, LEO satellites have attracted significant attention in NTN satellite communication research, owing to their relatively low path-loss effects resulting from their low orbital altitude and their cost efficiency in system deployment and operation.

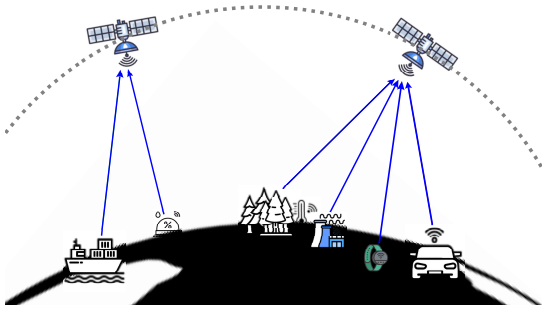

Fig. 1. System model of uplink multiple access in NTN-IoT networks, where heterogeneous IoT devices directly transmit data to LEO satellites.

Meanwhile, research in terrestrial IoT networks has progressively evolved to accommodate an explosive increase in devices while ensuring low latency. To this end, grant-free multiple access (GFMA) has been actively studied to reduce access delay by omitting the grant procedure. A notable advancement was the proposal of a resource-hopping based GFMA framework, which structures potential collisions using pre-assigned hopping patterns [4]. Subsequent studies provided a deeper understanding by rigorously and mathematically analyzing the fundamental impact of these resource collisions [5]. Furthermore, for scenarios where direct communication is unavailable, new cooperative non-orthogonal multiple access (NOMA) protocols leveraging relays in half-duplex relaying have been developed and analyzed with optimal joint decoding techniques [6]. More recently, research has advanced to opportunistic non-orthogonal random access (O-NORA), a technique that maximizes both reliability and efficiency by combining opportunistic transmission based on channel conditions with the theoretically optimal simultaneous non-unique decoding (SND) [7]. However, directly applying these advancements from terrestrial IoT networks to environments integrated with NTN presents several challenges [8].

These challenges are fundamentally twofold in LEO-IoT systems. First, resource-constrained IoT devices must efficiently cope with the physical limitations of satellite links, such as high mobility, frequent handovers, and long propagation delays. This device-side challenge is further exacerbated by the limited transmission power of IoT devices, which fails to effectively overcome the considerable path loss caused

by the long distance to the satellite, thereby degrading the received signal-to-noise ratio (SNR). Second, a single satellite must simultaneously support a vast number of sporadic and heterogeneous IoT devices within its wide coverage area. Therefore, this work focuses on developing efficient and reliable multiple access schemes to support large-scale IoT services in LEO satellite networks.

Fundamental multiple access schemes, namely time division multiple access (TDMA) and frequency division multiple access (FDMA), must pre-assign resources even to inactive IoT terminals with no data to transmit. Consequently, they cause considerable resource wastage in large-scale IoT environments characterized by sporadic traffic. While NOMA has been proposed as an alternative to address this resource inefficiency as considered in terrestrial IoT networks, its main variants remain unsuitable for the LEO-IoT environment [8]. For instance, power-domain NOMA in [9] requires precise transmit power control at each terminal to enable signal separation at the receiver, which imposes a substantial burden on IoT devices with limited power and computational resources [10]. Moreover, sparse code multiple access (SCMA), a form of code-domain NOMA [11], can hinder scalability in large-scale IoT terminal environments, as its complex multi-dimensional codebook structure induces significant system-wide management overhead. Meanwhile, the recently emerging rate-splitting multiple access (RSMA), a flexible interference management technique that splits messages into common and private parts to decode part of the interference while treating the rest as noise, has attracted considerable attention for next-generation communication networks due to its high spectral efficiency [12]–[14]. However, RSMA requires message splitting and sophisticated power allocation based on the channel state, making it impractical in the LEO-IoT environment, which is characterized by short data packets, strict power limitations, and rapidly varying channels. Therefore, conventional multiple access schemes fall short of adequately addressing the unique constraints of the LEO-IoT environment, highlighting the need for research on tailored multiple access techniques.

In this context, we revisit interleave-division multiple access (IDMA), which was originally proposed in terrestrial networks [15]. Unlike conventional multiple access schemes that rely on complex codebooks, IDMA distinguishes and multiplexes users through simple, user-specific interleaving. This streamlined structure eliminates the excessive overhead associated with designing and managing complex codebooks. Moreover, IDMA obviates the need for the channel-dependent and stringent power allocation required in power-domain NOMA, offering a critical advantage in the rapidly varying LEO satellite channels. As a result, transmitter complexity is significantly reduced, making IDMA well suited for low-cost and power-constrained IoT devices. In addition, the computational complexity of IDMA receivers scales linearly with the number of devices, thereby ensuring practical scalability for massive connectivity. Taken together, the simplicity, robustness, and scalability of IDMA make it a highly promising multiple access technique for effectively addressing the diverse challenges of LEO-IoT networks.

Accordingly, in this paper, we propose an orthogonal frequency division multiplexing (OFDM)-based IDMA scheme for LEO-IoT systems. Specifically, we adapt the conventional IDMA for TNs [15] to the high path-loss environment of LEO satellite communications by incorporating a repetition transmission mechanism, and we design an OFDM-based IDMA structure with channel coding to ensure compatibility with mobile communication standards. Furthermore, we rigorously evaluate the proposed OFDM-IDMA scheme through simulations under 3GPP NTN standard channel models. Extensive simulation results, analyzed in terms of bit error rate (BER) and frame error rate (FER), demonstrate that the proposed system achieves near-single-user performance through iterative decoding at the receiver, even in scenarios where multiple IoT devices directly connect to LEO satellites.

II. System Model and Assumptions

In this section, we investigate an uplink multiple access scenario where multiple IoT devices directly transmit data to a LEO satellite, as illustrated in Fig. 1. We consider M IoT devices equipped with a single antenna and a LEO satellite also equipped with a single antenna. In addition, to assess the performance of the multiple access scheme under controlled conditions, we assume that the distance between all IoT devices and the satellite is uniformly set to d km[1]. Furthermore, the main assumptions, channel models, and Doppler shift compensation for the proposed OFDM-IDMA scheme are presented below.

One of the most critical factors in the LEO communication environment is the Doppler shift, which results from the high relative velocity between the LEO satellite and ground terminals. A large Doppler shift induces a carrier frequency offset (CFO), which breaks the orthogonality among subcarriers in an OFDM system, thereby causing severe inter-carrier interference (ICI) and multiple access interference (MAI). According to the 3GPP technical report [17], a LEO satellite at an altitude of 600 km experiences a CFO of up to 48 kHz in the 2 GHz band and up to 720 kHz in the 30 GHz band. To address the Doppler shift, we assume that Doppler pre-compensation is performed, which is a commonly adopted approach in the literature [18]. When a terminal is equipped with a GNSS receiver, it can calculate and compensate for the required Doppler shift and timing advance for uplink transmission using its own location information and the satellite's ephemeris data. In contrast, for low-cost terminals without GNSS, the satellite computes a common compensation value based on the beam center and broadcasts it to all terminals. The residual frequency offset resulting from the differences in terminal locations, known as differential delay (DD), can then be managed on the network or at higher protocol layers [19]. In this paper, we assume that timing advance and frequency pre-compensation are successfully achieved through these mechanisms.

For link-level performance evaluation, we consider the standard 3GPP NTN channel models, namely the clustered

[1]In practical LEO satellite environments, the satellite-to-terminal distance can vary significantly depending on the terminal's geographical location and the satellite's elevation angle, leading to considerable differences in path loss. However, since LEO satellite communications typically serve multiple terminals through sharply focused beams, the distance differences among IoT devices within the same beam are sufficiently small [16].

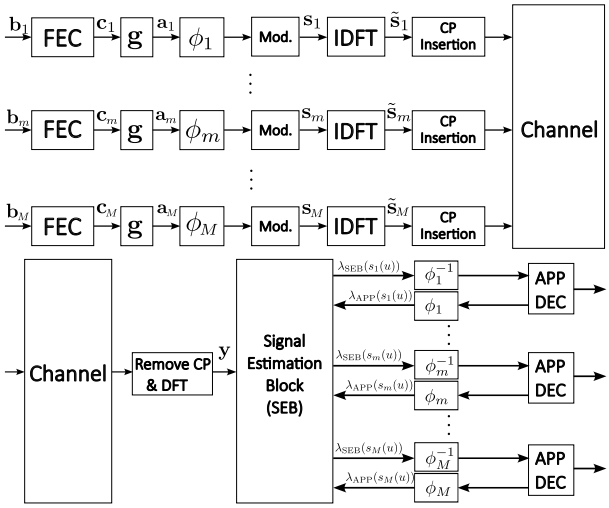

Fig. 2. Block diagram of the OFDM-IDMA systems

delay line (CDL) and tapped delay line (TDL) [20]. These models are designed to capture the unique characteristics of the NTN environment, including long propagation delays, high mobility, and significant Doppler shifts. The CDL model provides a detailed channel description that includes spatial parameters such as the angle of arrival (AoA) and angle of departure (AoD). While this is advantageous for analyzing multiple-input multiple-output (MIMO) systems with multiple antennas, the model is inherently complex and computationally expensive. In contrast, the TDL model simplifies the channel by employing a power delay profile (PDP) without spatial information, enabling efficient modeling of time-domain characteristics such as delay spread and Doppler spread.

As this study serves as a preliminary work focusing on an uplink system with a single-antenna configuration, we adopt the TDL model rather than analyzing the spatial properties of the channel. The TDL model offers low computational complexity while capturing key factors that critically affect the performance of the OFDM-IDMA system, such as propagation delays between the satellite and IoT devices. The detailed TDL channel parameters used in the simulations are described in Section V.

III. Overall Procedure of OFDM-IDMA

This section describes the basic procedure of OFDM-IDMA for NTN-based IoT networks. Fig. 2 illustrates the transmitter and receiver architecture of the proposed OFDM-IDMA system, where M IoT transmitters individually perform their transmissions. In this system, IoT devices multiplex their signals using device-specific interleavers, while the receiver performs iterative decoding N_{iter} times by parallelly decoding both interleaved and non-interleaved signals for each device, thereby benefiting from iterative multi-user detection to improve overall system performance. For the m-th device, the information bit sequence $\mathbf{b}_m (\in \{0,1\}^K)$ is encoded using forward error correction (FEC), where K denotes the number of information bits. In this paper, considering the constraints of low-power, low-cost IoT devices and their short-packet uplink transmissions, we adopt convolutional coding as the FEC scheme [5]. Then, $\mathbf{b}_m$ is encoded into a coded bit sequence $\mathbf{c}_m (\in \{0,1\}^Q)$ using a convolutional code with a code rate of $\rho_c (= K/Q)$.

Subsequently, to counteract the severe path loss inherent in LEO satellite links, the coded bit sequence $\mathbf{c}_m$ is expanded in the bit domain through $N\text{rep}$ repetitions. This procedure can be regarded as analogous to the spreading operation in code-division multiple access (CDMA). Specifically, based on the common masking sequence $\mathbf{g} (\in \{0,1\}^{N_{\text{rep}}})$, which is shared across the network and known to all nodes, $\mathbf{c}_m$ is spread to generate the bit sequence $\mathbf{a}_m (\in \{0,1\}^{QN_{\text{rep}}})$. The spreading rule is as follows: if the $q (\in \{1, 2, \cdots, Q\})$-th coded bit is $c_m(q) = 0$, it is spread using the sequence $\mathbf{g}$. If $c_m(q) = 1$, it is spread using the inverted version of the sequence $\mathbf{g}$. For example, let $\mathbf{c}_m = [0, 0, 1]$ and the masking sequence $\mathbf{g} = [0, 1, 0, 1]$. The first bit '0' is spread to [0, 1, 0, 1], and the second bit '0' is likewise spread to [0, 1, 0, 1]. The third bit '1' is spread to the inverted version of $\mathbf{g}$, i.e., [1, 0, 1, 0]. Consequently, the final spread coded sequence is $\mathbf{a}_m = [0, 1, 0, 1, 0, 1, 0, 1, 1, 0, 1, 0]$. As a result, the effective code rate of the system becomes $\rho = K/(QN_{\text{rep}})$. This output is passed through the device-specific interleaver ϕ_m. In this paper, we assume independent random interleavers with pairwise correlations that are nearly zero. And, the bit sequence is modulated according to the modulation order.

In this paper, we assume an OFDM system to ensure compatibility with mobile communication standards. Accordingly, the modulated symbol vector $\mathbf{s}_m$ is mapped onto N_{FFT} OFDM subcarriers for transmission. The difference between the number of symbols and subcarriers is compensated by zero padding. The time-domain transmit signal $\tilde{\mathbf{s}}_m$ is obtained through the inverse fast Fourier transform (IFFT) operation, and the signal at the $v (\in \{0, \cdots, N_{\text{FFT}} - 1\})$-th discrete-time sample, $\tilde{s}_m[v]$, is expressed as follows

$$\tilde{s}_m[v] = \sum_{n=0}^{N_{\text{FFT}}-1} s_m[n] e^{j2\pi \frac{n}{N_{\text{FFT}}} v}. \tag{1}$$

To maintain subcarrier orthogonality, the transmitted signal $\tilde{\mathbf{s}}_m^{\text{CP}} (\in \mathbb{C}^{N_{\text{FFT}}+N_{\text{CP}}})$ is constructed by inserting a cyclic prefix (CP) of length N_{CP}, obtained by copying the last N_{CP} samples of the OFDM block to its front. Here, N_{CP} is assumed to be longer than the channel impulse response. The LEO satellite receives a superposition of signals from M IoT devices. Each signal passes through the channel via linear convolution, and the resulting received signal vector $\tilde{\mathbf{y}} (\in \mathbb{C}^{N_{\text{FFT}}+N_{\text{CP}}+L-1})$, prior to CP removal, is expressed as follows[2]

$$\tilde{\mathbf{y}} = \sum_{m=0}^{M-1} \tilde{\mathbf{h}}_m \circledast \tilde{\mathbf{s}}_m^{\text{CP}} + \tilde{\mathbf{w}}, \tag{2}$$

where $\tilde{\mathbf{h}}_m \in \mathbb{C}^L$ is the L-tap channel impulse response vector between the m-th IoT device and the LEO satellite, $\circledast$ denotes the linear convolution operator, and $\tilde{\mathbf{w}} \sim \mathcal{CN}(\mathbf{0}, N_0\mathbf{I})$ is the corresponding additive white Gaussian noise vector.

[2]For ease of explanation, this paper assumes that the indexing of IoT devices starts from zero.

The LEO satellite removes the CP part from the time-domain received signal and performs an FFT operation, thereby obtaining the following frequency-domain signal.

$$\mathbf{y}(\in \mathbb{C}^{N_{\mathrm{FFT}}}) = \sum_{m=0}^{M-1} \mathbf{h}_m \circ \mathbf{s}_m + \mathbf{w}, \tag{3}$$

where $\mathbf{h}_m(\in \mathbb{C}^{N_{\mathrm{FFT}}})$ and $\mathbf{w}(\in \mathbb{C}^{N_{\mathrm{FFT}}})$ denote the channel response between the m-th IoT device and the LEO satellite and the noise vector in the frequency domain, respectively, while $\circ$ represents the Hadamard product, which is an element-wise multiplication. In the proposed OFDM-IDMA for LEO-IoT systems, all transmitted symbols on each subcarrier are detected according to the decoding method described later. Without loss of generality, this paper illustrates the detection procedure of the signal $s_m[u]$ transmitted by the m-th IoT device on an arbitrary u-th subcarrier, based on the received signal $y[u]$ corresponding to that subcarrier. Then, the received signal $y[u]$ is given by

$$y[u] = h_m[u]s_m[u] + z_m[u], \tag{4}$$

where

$$z_m[u] = \sum_{m' \neq m} h_{m'}[u]s_{m'}[u] + w[u]. \tag{5}$$

Under the assumption that a large number of devices simultaneously transmit signals, the given variable $z_m[u]$ can be approximated as a Gaussian random variable by invoking the central limit theorem. Resource-constrained IoT devices primarily employ low-order modulation schemes, and in this paper, we consider the case where an IoT device transmits quadrature phase shift keying (QPSK) symbols. Then, the transmitted symbol $s_m[u]$ for the m-th IoT device consists of a real part, $s_m^{\mathrm{Re}}[u]$, and an imaginary part, $s_m^{\mathrm{Im}}[u]$.

In QPSK modulation, we consider the detection of the real and imaginary components separately. To detect $s_m^{\mathrm{Re}}[u]$, $\mathrm{Re}(h_m^*[u]y[u])$ is used as a sufficient statistic. Accordingly, the likelihood function corresponding to the real part is given by

$$\begin{aligned} &p\left(\mathrm{Re}(h_m^*[u]y[u])|s_m^{\mathrm{Re}}[u] = \pm 1\right) \\ &= \frac{1}{\sqrt{2\pi \mathrm{Var}[\mathrm{Re}(h_m^*[u]z_m[u])]}} \\ &\times \exp\left(-\frac{\left(\mathrm{Re}(h_m^*[u]y[u] \mp |h_m[u]|^2 - \mathbb{E}[\mathrm{Re}(h_m^*[u]z_m[u]]\right)^2}{2\,\mathrm{Var}[\mathrm{Re}(h_m^*[u]z_m[u])]^2}\right) \end{aligned} \tag{6}$$

where $\mathbb{E}[\cdot]$ and $\mathrm{Var}[\cdot]$ denote the mean and variance, respectively.

IV. Receiver Architecture with Iterative Decoding

This section presents the receiver structure for the OFDM-IDMA system, which utilizes iterative decoding to effectively mitigate multi-user interference. The receiver consists of a signal estimation block (SEB) and an a posteriori probability (APP) decoder, which exchange soft decision information in each iteration. In this paper, based on [21], we assume that channel estimation at the receiver is error-free.

A. Signal Estimation Block (SEB)

Based on (6), the log-likelihood ratio (LLR) for $s_m^{\mathrm{Re}}[u]$ can be expressed as

$$\begin{aligned} &\lambda_{\mathrm{SEB}}[s_m^{\mathrm{Re}}[u]] \\ &= \frac{2|h_m[u]|^2 \left(\mathrm{Re}(h_m^*[u]y[u]) - \mathbb{E}[\mathrm{Re}(h_m^*[u]z_m[u])]\right)}{\mathrm{Var}[\mathrm{Re}(h_m^*[u]z_m[u])]}. \end{aligned} \tag{7}$$

Therefore, in (7), the statistics for the interference-plus-noise term $z_m[u]$ can be calculated as

$$\begin{aligned} &\mathbb{E}\left[\mathrm{Re}(h_m^*[u]z_m[u])\right] \\ &= h_m^{\mathrm{Re}}[u]\,\mathbb{E}[y^{\mathrm{Re}}[u]] + h_m^{\mathrm{Im}}[u]\,\mathbb{E}[y^{\mathrm{Im}}[u]] - |h_m[u]|^2\,\mathbb{E}[s_m^{\mathrm{Re}}[u]], \end{aligned} \tag{8}$$

$$\begin{aligned} &\mathrm{Var}\left[\mathrm{Re}(h_m^*[u]z_m[u]\right] \\ &= (h_m^{\mathrm{Re}}[u])^2\mathrm{Var}[y^{\mathrm{Re}}[u]] + (h_m^{\mathrm{Im}}[u])^2\mathrm{Var}[y^{\mathrm{Im}}[u]] \\ &\quad + 2h_m^{\mathrm{Re}}[u]h_m^{\mathrm{Im}}[u]\varphi[u]] - |h_m[u]|^4\mathrm{Var}[s_m^{\mathrm{Re}}[u]]. \end{aligned} \tag{9}$$

In (9), the covariance $\varphi[u]$ between $y^{\mathrm{Re}}[u]$ and $y^{\mathrm{Im}}[u]$ is given by

$$\varphi[u] = \sum_{m=0}^{M-1} h_m^{\mathrm{Re}}[u]h_m^{\mathrm{Im}}[u]\left[\mathrm{Var}[s_m^{\mathrm{Re}}[u]] - \mathrm{Var}[s_m^{\mathrm{Im}}[u]]\right]. \tag{10}$$

For the calculation of (8) and (9), the expectation of the received signal $y[u]$ can be decomposed into its real and imaginary parts as follows

$$\mathbb{E}\left[y^{\mathrm{Re}}[u]\right] = \sum_{m=0}^{M-1} \left(h_m^{\mathrm{Re}}[u]\,\mathbb{E}[s_m^{\mathrm{Re}}[u]] - h_m^{\mathrm{Im}}[u]\,\mathbb{E}[s_m^{\mathrm{Im}}[u]]\right), \tag{11}$$

$$\mathbb{E}\left[y^{\mathrm{Im}}[u]\right] = \sum_{m=0}^{M-1} \left(h_m^{\mathrm{Re}}[u]\,\mathbb{E}[s_m^{\mathrm{Im}}[u]] + h_m^{\mathrm{Im}}[u]\,\mathbb{E}[s_m^{\mathrm{Re}}[u]]\right), \tag{12}$$

Similarly, the variances of the real and imaginary parts of $y[u]$ can be expressed as

$$\begin{aligned} &\mathrm{Var}\left[y^{\mathrm{Re}}[u]\right] = \\ &\sum_{m=0}^{M-1} (h_m^{\mathrm{Re}}[u])^2\mathrm{Var}[s_m^{\mathrm{Re}}[u]] + (h_m^{\mathrm{Im}}[u])^2\,\mathrm{Var}[s_m^{\mathrm{Im}}[u]] + \frac{N_0}{2}, \end{aligned} \tag{13}$$

$$\begin{aligned} &\mathrm{Var}\left[y^{\mathrm{Im}}[u]\right] = \\ &\sum_{m=0}^{M-1} (h_m^{\mathrm{Im}}[u])^2\mathrm{Var}[s_m^{\mathrm{Re}}[u]] + (h_m^{\mathrm{Re}}[u])^2\,\mathrm{Var}[s_m^{\mathrm{Im}}[u]] + \frac{N_0}{2}. \end{aligned} \tag{14}$$

Finally, using the results of (8) and (9), we obtain (7). The LLR for the imaginary part, $s_m^{\mathrm{Im}}[u]$, is calculated through an identical procedure using $\mathrm{Im}(h_m^*[u]y[u])$.

B. A Posteriori Probability Decoder (APP)

In the APP decoder module, decoding is performed for each coded bit using the LLR values in (7) as input. Since the LLRs are computed independently for the real and imaginary parts, we first arrange them to form a unified bit sequence as follows:

$$\bar{\lambda}_{\mathrm{SEB}}[2u-1] = \lambda_{\mathrm{SEB}}[s_m^{\mathrm{Re}}[u]],\ \bar{\lambda}_{\mathrm{SEB}}[2u] = \lambda_{\mathrm{SEB}}[s_m^{\mathrm{Im}}[u]]. \tag{15}$$

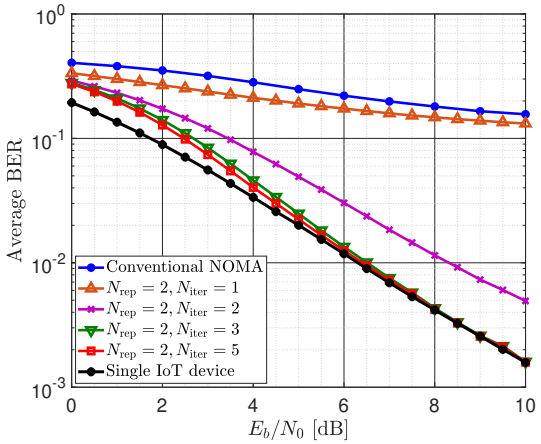

Fig. 3. BER performance of OFDM-IDMA in a LEO-IoT with four simultaneous devices ($M = 4$), comparison with conventional NOMA and single IoT device baseline

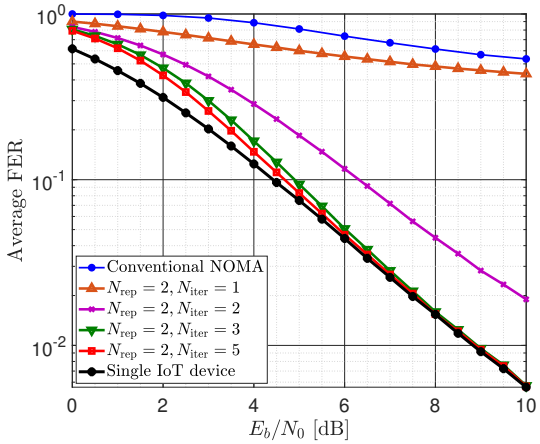

Fig. 4. FER performance of OFDM-IDMA in a LEO-IoT with four simultaneous devices ($M = 4$), comparison with conventional NOMA and single IoT device baseline

These LLRs are first deinterleaved by $\boldsymbol{\phi}_m^{-1}$. Afterwards, the deinterleaved LLRs of the repeatedly spread bit stream are despread. Since the LLR is defined as a real number, the operation is performed using the masking sequence $\hat{\mathbf{g}}(\in \mathbb{R}^{N_{\text{rep}}})$, which is obtained from the original masking sequence $\mathbf{g}$ by replacing bit 0 with 1 and bit 1 with -1, as follows.

$$\lambda[c_m[q]] = \sum_{j \in \mathcal{J}_m[q]} \hat{\mathbf{g}}[j] \phi_m^{-1} \left(\bar{\lambda}_{\text{SEB}}[j] \right), \tag{16}$$

where $\mathcal{J}_m[q]$ denotes the index set of the bits in the coded stream $\mathbf{a}_m$ that correspond to the q-th bit before repetition. The convolutional APP decoder takes $\lambda[c_m[q]]$ as input and computes the a posteriori LLRs for both coded and information bits. Subsequently, the LLRs of the information bits, $\lambda_{\text{APP}}[b_m[i]]$, are used to generate extrinsic feedback for the SEB. This feedback, denoted by $\lambda_{\text{APP}}[s_m^{\Lambda}[u]]$ where $\Lambda \in \{\text{Re}, \text{Im}\}$, is obtained by removing the original SEB contribution, i.e., intrinsic information, reapplying the masking sequence $\mathbf{g}$ and the interleaver ϕ_m to restore the SEB order. These extrinsic LLRs are converted into statistical measures such as mean and variance required by the SEB, and are then updated as follows

$$\mathbb{E}\left[s_m^{\Lambda}[u]\right] = \tanh\left(\frac{\lambda_{\text{APP}}[s_m^{\Lambda}[u]]}{2} \right), \tag{17}$$

$$\text{Var}\left[s_m^{\Lambda}[u]\right] = 1 - \left(\mathbb{E}[s_m^{\Lambda}[u]]\right)^2. \tag{18}$$

Subsequently, the updated $\mathbb{E}[s_m^{\Lambda}[u]]$ and $\text{Var}[s_m^{\Lambda}[u]]$ are used in (8) and (9) for the next SEB iteration. Finally, after N_{iter} iterations, hard decisions on the information bits are made directly by the APP decoder.

V. Simulation Results

In this section, we comprehensively evaluate and analyze the performance of the proposed OFDM-IDMA scheme for LEO-IoT systems. The performance is assessed in terms of BER and FER, and comparisons are made with the conventional NOMA scheme as well as a single IoT device environment without MAI. The simulation environment assumes an uplink scenario in which four IoT devices ($M = 4$) are simultaneously active. Each device transmits a frame consisting of $K = 60$ bits.

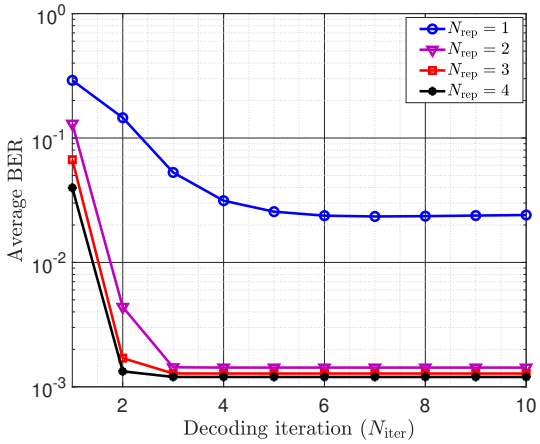

Fig. 5. BER convergence characteristics according to repetition count (N_{rep}) and receiver iteration count (N_{iter}) in an OFDM-IDMA system

The channel coding scheme employs a convolutional code with a code rate of $\rho_c = 1/3$, a constraint length of 9, and an octal generator polynomial of [557,663,711], which is further combined with a repetition code of factor N_{rep}. QPSK modulation is applied, and the number of receiver iterations for the SEB and APP decoding process is denoted by N_{iter}. The physical layer is based on OFDM with a subcarrier spacing (SCS) of 15 kHz, an FFT size of 2048, and a CP length equal to $1/16$ of the FFT size. For the satellite channel model, the NTN-TDLC5 model defined in the 3GPP standard [22] is adopted, which features a delay spread of 5 ns with two delay taps.

Figs. 3 and 4 present the average BER and FER performance with respect to E_b/N_0. In this case, the repetition factor is fixed at $N_{\text{rep}} = 2$, while the number of receiver iterations (N_{iter}) is set to 1, 2, 3, and 5. For the conventional NOMA scheme, the performance deteriorates due to insufficient mitigation of MAI under severe path loss. The OFDM-IDMA system also shows degraded performance at $N_{\text{iter}} = 1$, since MAI is not adequately suppressed. However, as the number of iterations increases, the performance improves significantly, and with $N_{\text{iter}} = 5$, the BER and FER performance closely approaches that of the single-device case. These results clearly demonstrate that the iterative decoding mechanism of the

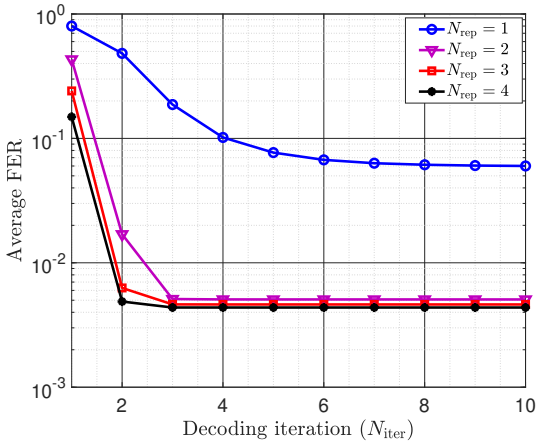

Fig. 6. FER convergence characteristics according to repetition count (N_{rep}) and receiver iteration count (N_{iter}) in an OFDM-IDMA system

OFDM-IDMA receiver is highly effective for supporting multiple access in an LEO-IoT environment.

Figs. 5 and 6 illustrate the convergence characteristics of BER and FER with respect to the number of receiver iterations (N_{iter}) at $E_b/N_0 = 10$ dB. The BER and FER performance saturates rapidly with only a small number of iterations, and when $N_{\text{rep}} \geq 2$, most of the performance improvement is achieved within the first 3–4 iterations. This fast convergence provides a significant advantage in terms of computational complexity and power consumption for IoT devices. In other words, near-optimal performance can be attained with only a few iterations, implying that IDMA technology can be efficiently applied to resource-constrained IoT devices.

VI. Conclusion

In this paper, we proposed and comprehensively evaluated an OFDM-IDMA system as a robust multiple access solution for LEO satellite-based IoT networks. Considering the inherent challenges of NTNs, including severe path loss and the requirement to support a massive number of low-power IoT devices, we introduced an IDMA framework that combines spreading and FEC, and applied an OFDM-based transceiver architecture along with a standardized NTN channel model to ensure compatibility with mobile communication standards. Simulation results demonstrated that the proposed OFDM-IDMA technique achieved clear superiority over the conventional scheme in the LEO-IoT uplink scenario, and that multiple access performance could approach the single-device bound with only a few receiver decoding iterations.

Acknowledgment

This work was supported in part by the Institute for Information and Communications Technology Planning & Evaluation (IITP) Grant funded by the Korea Government (MSIP, Development of Cube Satellites Based on Core Technologies in Low Earth Orbit Satellite Communications) under Grant RS-2024-00396992 and in part by the the National Research Foundation of Korea (NRF) through the Korean Government (MSIT) under Grant No. RS-2025-02303435.

References

[1] L. Chettri and R. Bera, "A comprehensive survey on Internet of Things (IoT) toward 5G wirelesss systems?," *IEEE Internet Things J.*, vol. 7, no. 1, pp. 16–32, Jan. 2020.

[2] IoT Analytics, "State of IoT 2024: Number of connected IoT devices growing 13% to 18.8 billion globally." [Online]. Available: https://iot-analytics.com/number-connected-iot-devices/.

[3] A. Ramirez-Arroyo, T. B. Sorensen, and P. Mogensen,"Terrestiral 5G and Starlink NTN multi-connectivity toward 6G communications integration era: An empirical assessment," *IEEE Open J. Commun. Soc.*, vol. 6, pp. 5269–5283, Jun. 2025.

[4] H. S. Jang, B. C. Jung, T. Q. S. Quek, and D. K. Sung, "Resource-hopping based grant-free multiple access for 6G-enabled massive IoT networks," *IEEE Internet Things J.*, vol. 8, no. 20, pp. 15349–15360, Oct. 2021.

[5] Y. -S. Lee, K. -H. Lee, H. S. Jang, G. Jo, and B. C. Jung, "Performance analysis of resource-hopping based grant free multiple access for massive IoT networks," *IEEE Wireless Commun. Lett.*, vol. 11, no. 12, pp. 2685–2689, Dec. 2022.

[6] J. S. Yeom, Y. -B. Kim, and B. C. Jung, "Spectrally efficient uplink cooperative NOMA with joint decoding for relay-assisted IoT networks," *IEEE Internet Things J.*, vol. 10, no. 1, pp. 210–223, Jan. 2023.

[7] J. S. Yeom and B. C. Jung, "Opportunistic non-orthogonal random access with optimal decoder for 6G multi-channel IoT networks," *IEEE Wireless Commun. Lett.*, vol. 14, no. 7, pp. 2264–2268, Jul. 2025.

[8] T. T. T. Le, N. U. Hassan, X. Chen, M.-S. Alouini, Z. Han, and C. Yuen, "A survey on random access protocols in direct-access LEO satellite-based IoT communication," *IEEE Commun. Surveys Tuts.*, vol. 27, no. 1, pp. 426–462, Feb. 2025.

[9] F. A. Tondo, J. M. d. S. Sant'Ana, S. Montejo-Sánchez, O. L. A. López, S. Céspedes, and R. D. Souza, "Non-orthogonal multiple access strategies for direct-to-satellite IoT networks," *IEEE Trans. Aerosp. Electron. Syst.*, early access, Aug. 04, 2025.

[10] J. Jeong, H. Lee, and D. Hong, "Enhanced early preamble collision detector for LEO satellite based NTN IoT random access," *IEEE Trans. Veh. Technol.*, vol 74, no. 8, pp. 12496–12511, Aug. 2025.

[11] Y. Liu, c. Zhang, J. Hu, J. Chen, and K. Yang, "Low-complexity MIMO-SCMA detection for LEO satellite communications," *IEEE Trans. Veh. Technol.*, vol. 74, no. 3, pp. 5253–5258, Mar. 2025.

[12] W. U. Khan, *et al.*, "Rate splitting multiple access for next generation cognitive radio enabled LEO satellite networks," *IEEE Trans. Wireless Commun.*, vol. 22, no. 11, pp. 8423–8435, Nov. 2023.

[13] J. Ryu, A. Kaushik, B. Lee, and W. Shin, "Rate-splitting multiple access for GEO-LEO coexisting satellite systems: A traffic-aware throughput maximization precoder design," *IEEE Trans. Veh. Technol.*, vol. 73, no. 12, pp. 19838–19843, Dec. 2024.

[14] K. Wang, X. Wang, N. Zhao, X. Yang, H. Fang, and D. Niyato, "Uplink RSMA in LEO satellite communications: A perspective from generative artificial intelligence," *IEEE Trans. Veh. Technol.*, early access, Jun. 17, 2025.

[15] L. Ping, L. Liu, K. Wu, and W. K. Leung, "Interleave division multiple access," *IEEE Trans. Wireless Commun.*, vol. 5, no. 4, pp. 938–947, Apr. 2006.

[16] D. Kim, H. Jung, I. -H. Lee, and D. Niyato, "Multibeam management and resource allocation for LEO satellite-assisted IoT networks," *IEEE Internet Things J.*, vol. 12, no. 12, pp. 19443–19458, Jun. 2025.

[17] 3GPP TR 38.811, "Technical Specification Group Radio Access Networks; Study on New Radio (NR) to support non-terrestrial networks (Release 15)," v.15.4.0, Sep. 2020.

[18] H. Chougrani, S. Kisseleff, W. A. Martins, and S. Chatzinotas, "NB-IoT random access for nonterrestrial networks: Preamble detection and uplink synchronization," *IEEE Internet Things J.*, vol. 9, no. 16, pp. 14913–14927, Aug. 2022.

[19] 3GPP TR 38.821, "Technical Specification Group Radio Access Networks; Solutions for NR to support non-terrestrial networks (NTN) (Release 16)," v.16.2.0, Apr. 2023.

[20] 3GPP TR 38.901, "Technical Specification Group Radio Access Networks; Study on channel model for frequencies from 0.5 to 100 GHz (Release 18)," v.18.0.0, Mar. 2024.

[21] K.-X. Li, X. Gao, and X.-G. Xia, "Channel estimation for LEO satellite massive MIMO OFDM communications," *IEEE Trans. Wireless Commun.*, vol. 22, no. 11, pp. 7537–7550, Nov. 2023.

[22] 3GPP TR 38.108, "Technical Specification Group Radio Access Networks; NR; Satellite access node radio transmission and reception (Release 19)," v.19.1.0, Jun. 2025.